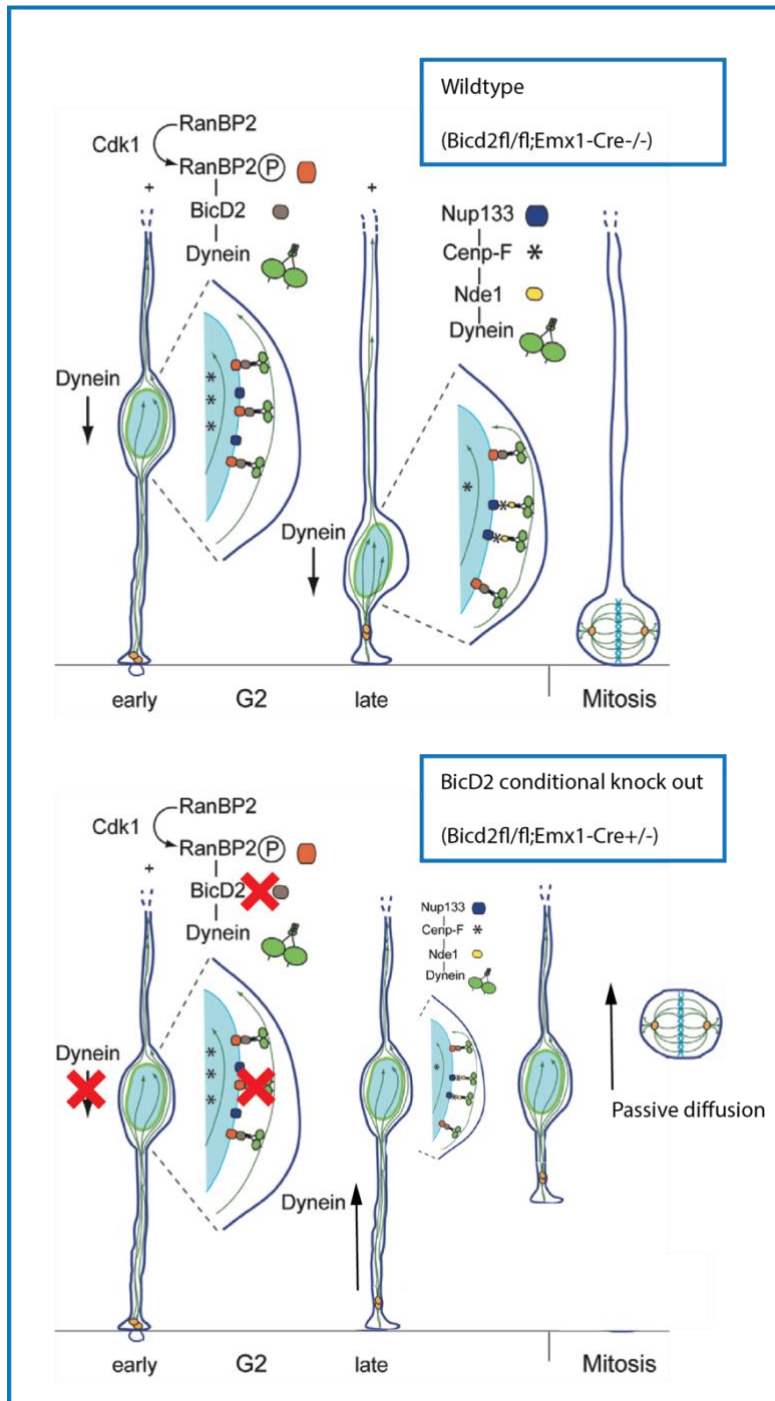


BicD2 Controls Cell Cycle-Dependent Positioning of Neural Stem cells

Graphical Abstract



Adapted from Bertipaglia et al., 2017

Author

Jasper van Schelt

Correspondence

j.j.schelt@students.uu.nl

First Assessor

Lena Will

Second Assessor

Esther de Graaff

Summary

In the embryo millions of cells are produced and form the incredibly complex structure of the brain. Neural stem cells are the parents of almost all other cells in the brain. Brain development is instructed by the genetic code in all cells. Changes in this genetic code are called mutations and can lead to brain malformations in patients. One of these mutations was found in the genetic code of BicD2. This study aims to understand what role BicD2 plays in neural stem cells during brain development. I used a technique to specifically remove BicD2 in the neural stem cells of mice. Neural stem cells are normally attached to the inner surface of the brain and only divide at a specific place. I found that neural stem cells without BicD2 were no longer attached to the surface and started dividing at other places within the brain. This work will help us to understand in more detail how the brain is made in the embryo and how this process is affected in patients with mutations in BicD2.





Internship Report

BicD2 Controls Cell Cycle-Dependent Positioning of Neural Stem Cells During Neocortical Development

Jasper van Schelt

Faculty of Science, Cell Biology, Neurobiology and Biophysics, Utrecht University, 3584CH, Utrecht, The Netherlands

Correspondence: j.j.schelt@students.uu.nl

SUMMARY

Radial Glial Progenitors (RGPs) are elongated epithelial cells and are the primary progenitor cell during development of the mammalian neocortex. The RGP cell-cycle and nuclear migration within the ventricular zone (VZ) are tightly interdependent and misregulation of these processes can cause severe neurodevelopmental disorders. Previous knock down studies showed that the dynein activating adaptor protein BicD2 is essential for RGP nuclear migration and mitotic entry. However, the precise *in vivo* role of BicD2 in RGPs remains unclear. By comparing cell-type specific BicD2 conditional knockout mice, we found the location but not the number of mitotic progenitors was altered. Instead of entering mitosis strictly at the ventricular surface (VS), RGP now entered mitosis across the VZ. Analysis of chromatin morphology, cell morphology and the location of the nuclei and centrosomes suggest these cells are present in two distinct populations. One population appears to be halted in their mitotic progression and nuclear migration while the other is released from the VS and continues through mitosis. Altered RGC morphology is further supported by experiments using organotypic slice culture after *ex vivo* brain electroporation at early stages of development. Furthermore, immunostaining against BicD2 showed a punctate pattern at the VS and often localized to anti-Pericentrin positive punctae, hinting at additional functions of BICD2 in RGP. Together my data demonstrates surprising effects of BicD2-depletion in RGPs providing new insights into BicD2's role in the development of the mammalian neocortex.

INTRODUCTION

The complex process of neocortical development is initiated within a zone of rapidly proliferating radial glial progenitor cells (RGPs) (Noctor et al., 2004). They form a pseudostratified epithelium spanning the neural tube from the apical ventricular surface (VS) to the basal pial surface (PS). RGP cell-cycle and nuclear positioning is tightly co-regulated in a process called interkinetic nuclear migration (INM) (Sauer, 1935). RGPs undergo S-phase when the nucleus is in the outer VZ (oVZ), while during G2 the nucleus migrates apically and divides when it reaches the VS. Initially RGPs divide symmetrically but progressively switch to asymmetric divisions producing one daughter cell that is destined to become a neuron (Kriegstein & Alvarez-Buylla, 2009). Neurons subsequently migrate radially outward passing through earlier born neurons forming the laminated structure of the adult neocortex (Noctor et al., 2001).

The microtubule (MT) cytoskeleton plays essential roles in both RGPs and developing neurons, and numerous human mutations in MT-associated genes have been found to cause severe neurodevelopmental pathologies. One of these proteins is the dynein activating adaptor protein Bicaudal-D2 (BicD2). Mutations in BicD2 can cause

SMALED2A, a dominant mild early onset form of spinal muscular atrophy (Neveling et al., 2013; Peeters et al. 2013). More recently, BicD2 mutations have also been associated with malformations of cortical development (MCD). A mutation in the cargo binding domain of BicD2 (R694C) causes polymicrogyria and cerebellar hypoplasia (Ravenscroft et al., 2016). In addition, a C-terminal truncating mutation (K775Ter) was found in a patient with lissencephaly, subcortical band heterotopia and mild hydrocephalus (Tsai et al., 2020). BicD2 functions in dynein recruitment to the nucleus by binding the nuclear envelope proteins RanBP2 (Splinter et al. 2010) and Nesprin-2 (Goncalves et al., 2020). In addition, BicD2 functions in the MT-dependent transport of secretory vesicles through Rab6 binding (Grigoriev et al., 2007; Splinter et al., 2012). Recent rodent studies have elucidated how these molecular functions contribute to cellular behavior during brain development. BicD2 knockout (KO) mice showed severe lamination defects in the neocortex and cerebellum associated with complications during neuronal migration (Jaarsma et al., 2014). In the cerebellum neuronal migration defects were entirely dependent on expression of BicD2 in progenitors. A series of studies using *in utero* electroporation (IUE) to knockdown (KD) or introduce specific genes elucidated

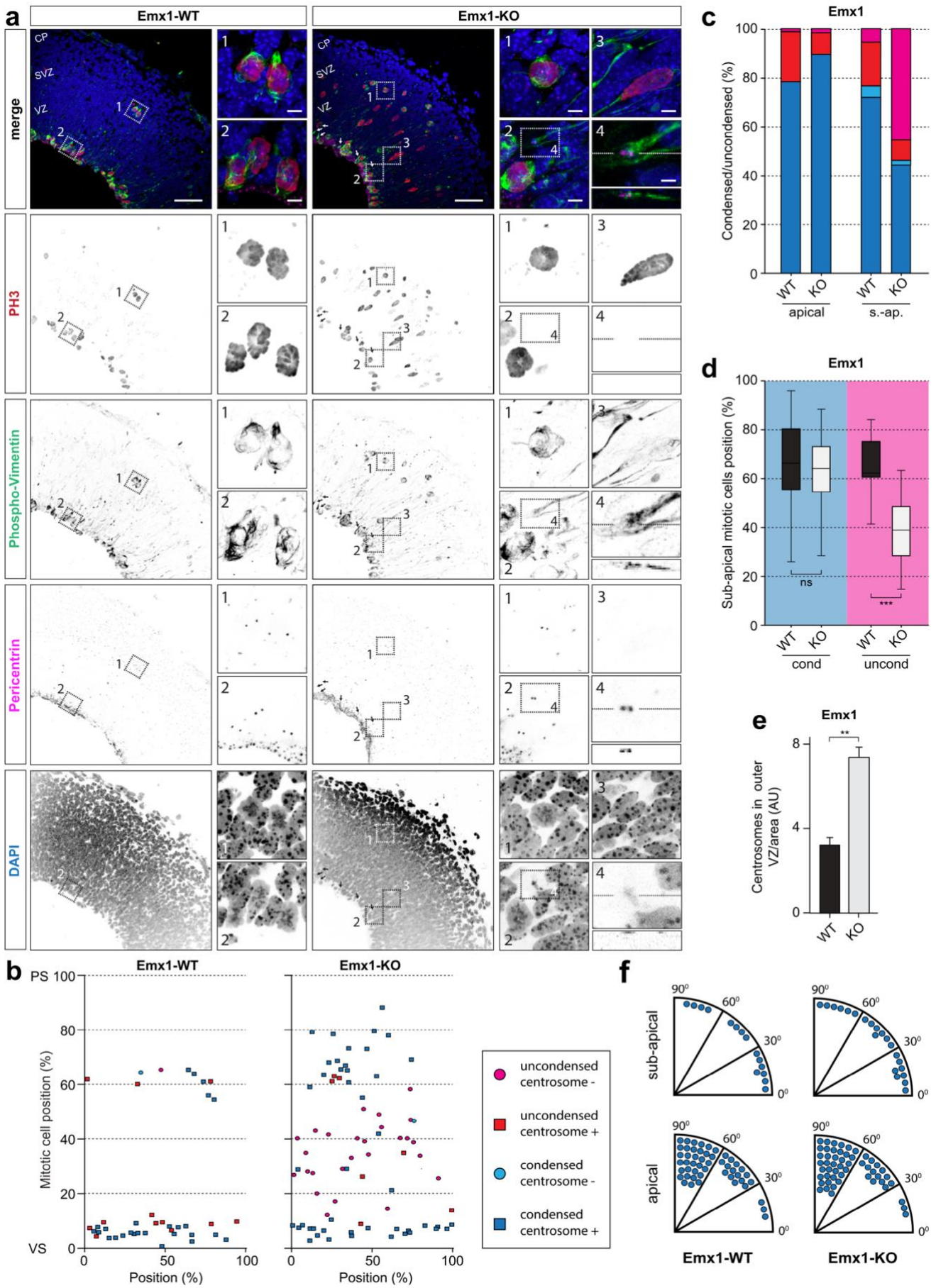


Figure 1. See legend on next page

the role of MTs and BicD2 in RGP of the neocortex. In RGP MTs nucleate from the centrosomes anchored at the VS and grow around the nucleus in the basal direction forming a highly polarized array (Tsai et al., 2010). During G2, RanBP2 phosphorylation by Cdk1 induces binding of BicD2 and recruitment of dynein, stimulating apical nuclear migration (Hu et al., 2013; Baffet et al., 2015). Just before the nucleus reaches the VS, the centrosomes move towards the nucleus and separate to form the mitotic spindle. Importantly, these studies showed that blocking apical nuclear migration by BicD2 KD prevents mitotic entry in RGPs.

These results suggest cortical defects in BicD2 KO mice and in patients with BicD2 mutations are caused by altered BicD2 function in RGPs. However, because RGPs give rise to neurons and function as a scaffold during neuronal migration, it has remained unclear to what extent cortical defects arise from BicD2 depletion in RGPs or neurons. Therefore, Will et al. made use of cell-type specific conditional KO (cKO) mouse lines (Will et al., 2019). Emx1-driven BicD2 cKO (Emx1-KO), which are BicD2-deficient in RGPs and post-mitotic neurons, were compared with Nex-driven BicD2 cKO mice (Nex-KO), which are BicD2-deficient only in post-mitotic neurons. Nex-KO mice showed severe lamination defects indicating that the affected neuronal migration is dependent on BicD2 depletion in neurons. Single-neuron labeling and rescue experiments using *ex-vivo* electroporation (EVE) revealed that BicD2 works in a cell intrinsic manner during the bipolar locomotion mode. Surprisingly however, little difference in neuronal production was observed between Emx1-KO and Nex-KO. In addition, a slight but not significant increase in mitotic cells was observed in Emx1-KO. These results are surprising given previous BicD2 kd studies where BicD2 deficient RGPs are arrested in G2. It remains unclear how these progenitors can enter mitosis and produce the observed number of neurons.

To further examine mitosis in RGPs, I made use of immunostaining in Emx1-KO and WT mice. Here I report that Emx1-KO mice show altered position and cell-cycle

progression of mitotic RGPs. Simultaneous quantification of chromatin morphology, nuclear location and centrosome location revealed that mitotic RGPs are present in two populations, a progressing delaminated state and a non-progressing state. Cell labeling using organotypic slice culture after EVE at early stages of development further suggests an altered RGP morphology. Immunostaining against BicD2 and Pericentrin in WT revealed BicD2 immunoreactivity shows a punctate pattern at the VS in proximity to Pericentrin-positive punctae, potentially pointing to unknown roles for BicD2 in RGPs. Together, these results suggest BicD2-deficient RGPs delaminate from the VS allowing them to progress through mitosis because of the proximity of their centrosomes. This study provides insights into the role of BicD2 in RGPs that are of key importance for further investigation of BicD2 associated neurodevelopmental pathologies.

RESULTS

BicD2 depletion in RGPs alters the position and cell cycle progression of mitotic progenitors

To test the distribution and cell-cycle progression of mitotic RGPs, I performed immunostaining on E14.5 Emx1-WT (*Bicd2^{fl/fl};Emx1-Cre^{-/-}*) and Emx1-KO (*Bicd2^{fl/fl};Emx1-Cre^{-/+}*) mice (Fig.1A). Using Phospho-Histone H3 (PH3) a marker for mitotic nuclei, I found WT RGPs mainly entered mitosis at the VS and rarely at sub-apical locations in the subventricular zone (SVZ). In KO however, a massive increase was observed of PH3+ RGPs at sub-apical locations. To investigate mitotic progression, I analyzed the chromatin morphology using DAPI staining. During interphase and early prophase chromatin is in an uncondensed (cond-) state while condensed chromatin (cond+) is present during late-prophase and later phases of mitosis. Therefore, the percentage of cond+ can be used to measure mitotic progression. Cond- chromatin can be identified by spots of intense DAPI staining distributed uniformly across the nucleus while cond+ cells have more intense DAPI staining in the center surrounded by DAPI

Figure 1. The role of BicD2 in mitotic progression and centrosome locations in RGPs

(A) Coronal cryo-sections of E14.5 cortices from Emx1-WT and Emx1-KO mice. Sections were stained with the DNA marker DAPI (blue), the centrosome marker Pericentrin (magenta) and the mitotic markers Phospho-Vimentin (green) and Phospho-Histone H3 (PH3, red). Centrosomes within apical processes of sub-apical mitotic progenitors are observed (arrows). Zooms showing location of centrosomes and chromatin condensation in apical and sub-apical mitotic cells. Emx1-WT + Emx1-KO: Zoom 1: condensed subapical dividing cells with centrosomes. Zoom 2: apical mitotic cells with condensed chromatin and centrosomes. Emx1-KO: Zoom 3: sub-apical mitotic cell with uncondensed chromatin and without centrosomes. Zoom 4: detached apical process containing centrosomes of mitotic cell in Zoom 3. Scale bars are 50 μ m for overview, 5 μ m for panels 1–3, and 2 μ m for panel 4.

(B) Distribution of mitotic cells with condensed or uncondensed chromatin, and with or without perinuclear centrosomes, as relative position over the cortical longitude from VS to PS (in %).

(C) Quantification of chromatin condensation and perinuclear centrosomes in apical and sub-apical mitotic cells (in %) (N = 5–6, n = 15–50).

(D) Relative position of sub-apical mitotic cells with condensed or uncondensed chromatin, over the cortical longitude from VS to PS (in %) (N = 5–6, n = 15–50).

(E) Number of centrosomes per area in the outer VZ (N = 6–7, n = 10–80).

(F) Cleavage plane orientation relative to the VS based on Pericentrin and DAPI staining in apical and sub-apical mitotic cells. CP: cortical plate, PS: pial surface, SVZ: subventricular zone, VS: ventricular surface, VZ: ventricular zone. s.-ap: sub-apical. *** p < 0.001, ** p < 0.005, ns = not significant; error bars are \pm SEM. Used tests: Kruskal Wallis test with Dunn's multiple comparisons (d), unpaired t-test (e)

staining with less intensity (Fig.1A). At the VS in both Emx1-WT and Emx1-KO, PH3+ RGP had mostly condensed chromatin (79% in Emx1-WT vs 93% in Emx1-KO) (Fig.1C). This percentage for sub-apical PH3+ RGP was very similar in Emx1-WT (77%). Surprisingly, in Emx1-KO sub-apical mitotic RGP chromatin condensation was drastically decreased (46%), suggesting that cell-cycle progression of BicD2-depleted sub-apical mitotic RGP is impaired. These data suggest that BicD2-depleted RGP enter mitosis at ectopic sub-apical locations and, specifically these but not VS dividing RGP, are impaired in their mitotic progression.

Sub-apical mitotic progenitors are present in two distinct states with different morphology and positioning of the nucleus and centrosome

Looking at chromatin condensation, I noticed RGP with impaired mitotic progression appear to have a more elongated morphology than other mitotic RGP. To further investigate the morphology of these cells, I performed anti-Phospho-Vimentin (PV) immunostaining. Vimentin is an intermediate filament which is present in a phosphorylated state specifically during mitosis, allowing the visualization of cytoplasm surrounding mitotic nuclei. PV staining showed radial processes in the VZ in both Emx1-WT and Emx1-KO (Fig.1A). However, only in Emx1-KO and only in sub-apical PH3+/cond- RGP these processes could be observed on the apical side of the corresponding nucleus (Fig.1A, Emx1-KO, Zoom 3). Because the centrosome plays a crucial role in RGP morphological integrity, I visualized the centrosomes using anti-Pericentrin staining.

Combining this with PV allowed me to match the centrosome to mitotic nuclei when the centrosomes were proximal to the nucleus. Quantification of the proximity of centrosomes to mitotic nuclei revealed that only in Emx1-KO PH3+/cond- RGP, most nuclei lacked proximal centrosomes (85%) (Fig.1C). Centrosomes near the VS were often located within apical processes of mitotic cells (Fig.1A, arrows). Because PV staining was not continuous throughout the cell, I could not match most of these centrosomes within apical processes to mitotic nuclei. However, the absence of a corresponding nucleus at the VS strongly suggests that the nucleus is located more distantly at sub-apical locations. Indeed, for some RGP PV staining visualized a continuous process from the centrosome to the nucleus (Fig.1, Emx1-KO, Zoom 2,3,4). Together, these data show that in KO the sub-apical progressing RGP have perinuclear centrosomes while in non-progressing subapical RGP the centrosomes are located within apical processes at larger distance from the nucleus.

Since centrosomes and the MT cytoskeleton are essential for the maintenance of RGP attachment to the VS (Insolera et al., 2014), I hypothesized that cond+ sub-apical RGP in KO can progress through mitosis because they are released from the VS and consequently have proximal centrosomes. Because detachment from the VS is thought to lead to a passive displacement to the oVZ, I subsequently analyzed the position of cond- vs cond+ mitotic nuclei. Indeed, in Emx1-KO PH3+/cond+ RGP were located at larger distances from the VS than PH3+/cond- RGP (Fig.1D). Furthermore, the number of centrosomes within the VZ at sub-apical locations was

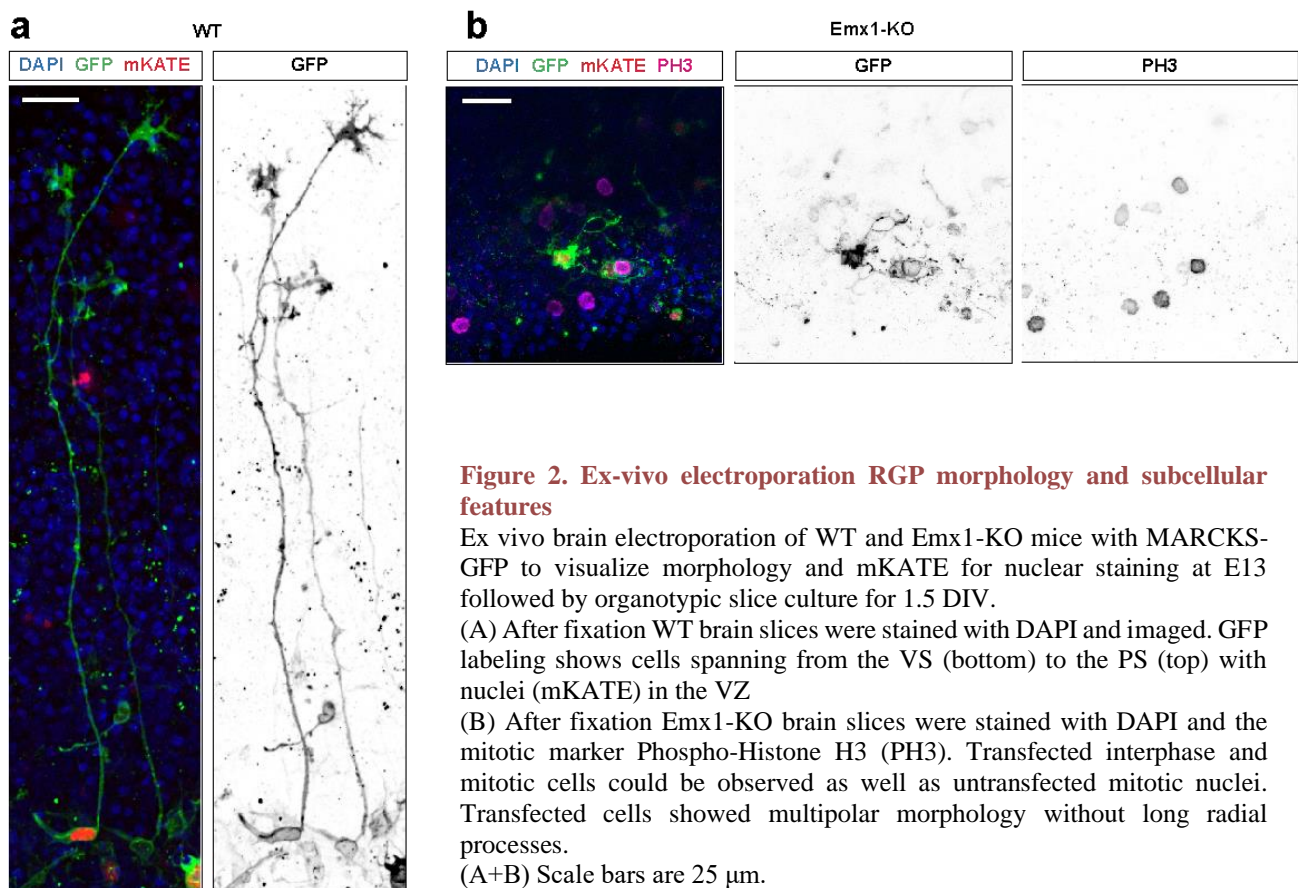


Figure 2. Ex-vivo electroporation RGP morphology and subcellular features

Ex vivo brain electroporation of WT and Emx1-KO mice with MARCKS-GFP to visualize morphology and mKATE for nuclear staining at E13 followed by organotypic slice culture for 1.5 DIV.

(A) After fixation WT brain slices were stained with DAPI and imaged. GFP labeling shows cells spanning from the VS (bottom) to the PS (top) with nuclei (mKATE) in the VZ

(B) After fixation Emx1-KO brain slices were stained with DAPI and the mitotic marker Phospho-Histone H3 (PH3). Transfected interphase and mitotic cells could be observed as well as untransfected mitotic nuclei. Transfected cells showed multipolar morphology without long radial processes.

(A+B) Scale bars are 25 μm.

more than doubled in Emx1-KO compared to Emx1-WT, suggesting that BicD2 is indeed required for centrosome attachment at the VS. Delamination of RGP can occur when RGP divide with a tilted cleavage plane (Shitamukai et al., 2011). However, no change was observed in the cleavage plane orientation of BicD2 depleted RGP (Fig.1F). Together, these data suggest RGP detach from the VS through mechanisms unrelated to cleavage plane orientation and move with their centrosomes to the outer VZ where they continue to divide.

EVE can be used as a tool to investigate morphology and subcellular features of RGP

Single-cell labeling with co-staining can provide more precise information on cell morphology and subcellular organization. EVE and organotypic slice culture have proven to be effective techniques for single-cell labeling in developing neurons (Will et al., 2019). However, to analyze mitosis in RGP, EVE needs to be performed at earlier stages of development when mouse brains are significantly smaller and more fragile. To this end, I performed pilot experiments using EVE at E13 with mKate and MARCKS-GFP to label the nuclei and the membrane of transfected cells respectively. After 1.5 days of organotypic slice culture, allowing fluorescent reporter expression, I fixed and image the slices. In WT, RGC could be observed spanning from the VS to the PS with their nuclei within the VZ (Fig.2A). Using the same experimental setup with additional immunolabeling after fixation I stained for PH3 in Emx1-KO. PH3+ nuclei could be observed in transfected and untransfected cells at sub-apical locations (Fig.2B). Transfected PH3+ and PH3-

cells within the VZ appeared to be unpolarized with no clear apical or basal process. These data suggest mitotic BicD2 depleted RGP at sub-apical locations are released from the VS and PS.

BicD2 immunoreactivity shows a punctate pattern at the VS adjacent to Pericentrin-positive punctae

In addition to functioning at the nuclear envelope, BicD2 controls the movement of secretory vesicles through Rab6 binding (Grigoriev et al., 2007; Splinter et al., 2012). Therefore, I investigated the localization of BicD2 in WT RGP using immunostaining. I used anti-BicD2 antibodies which were tested on Emx1-KO and Nex-KO sections and shown to be specific for BicD2 (Will et al. 2019). Consistent with previous reports (Hu et al., 2013), anti-BicD2 immunostaining localizes around RGP nuclei in the VZ (Fig.3). Additionally, BicD2-immunoreactivity was observed in a punctate pattern at the VS. Co-staining with Pericentrin showed BicD2-positive punctae often localized adjacent, and mostly apical to Pericentrin-positive punctae at the VS. (Fig.3, Zoom 3). Additionally, pericentrosomal BicD2 positive punctae were observed in mitotic cells (Fig.3, Zoom 1+2). Interestingly, anti-BicD2 positive punctae were usually associated with just one of the centrosomes in mitotic cells. These findings suggest additional unexplored roles for BicD2 in RGP.

DISCUSSION

In this study, I show that BicD2 depletion in RGP causes altered positioning of mitotic RGP to sub-apical locations. A subpopulation of these sub-apical mitotic RGP were

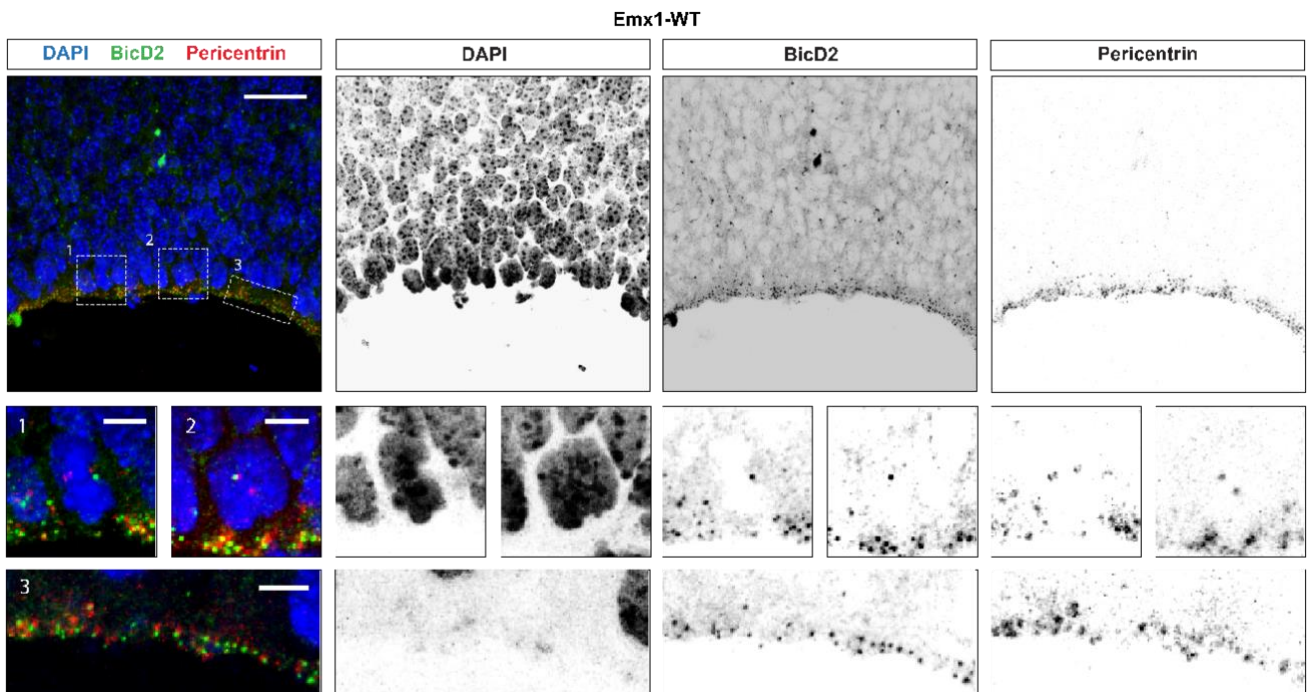


Figure 3. BicD2 localization at the ventricular surface with respect to centrosomes

Coronal cryo-sections of E14.5 cortices from Emx1-WT mice. Sections were stained with the DNA marker DAPI (blue), BicD2 (green) and the centrosome marker Pericentrin (red). Pericentrosomal BicD2 punctate staining can be observed at the VS apically to Pericentrin (Zoom 3) and in mitotic cells in association with one of the two centrosomes (Zoom 1+2). Scale bar is 25 μm in overview and 5 μm in zooms.

impaired in mitotic progression and lacked perinuclear centrosomes. In contrast to the effects of BicD2 KD however, RGPs at the VS and sub-apical RGPs with perinuclear centrosomes can progress through mitosis. Furthermore, BicD2 is essential for RGP attachment to the VS *in vivo*. Our results indicate that BicD2-depleted RGPs detach from the VS and continue to divide in the outer VZ in the presence of perinuclear centrosomes.

Role of BicD2 in RGP proliferation *in vivo*

BicD2 KD prevented mitotic entry in RGPs (Hu et al., 2013). Here I show that mitotic entry is not impaired in RGPs after BicD2 cKO. Additional mechanisms exist for RGP apical nuclear migration (Hu et al., 2013), which might compensate for cKO of BicD2 but not for the acute loss of BicD2 after KD. Furthermore, KD causes BicD2 loss of function in single cells which need to compete with surrounding WT RGPs for nuclear migration to the VS. In cKO, all RGPs are BicD2 depleted and are therefore in a more equal competition with surrounding nuclei when migrating to the VS. This could explain my observation of mitotically progressing RGPs at the VS in Emx1-KO mice. In the outer VZ, mitotically impaired PH3+ RGPs were observed lacking perinuclear centrosomes. These RGPs in cKO might be able to enter mitosis but delayed. This would not be observed after BicD2 KD because of the short time frame of these experiments.

Mitotically progressing RGPs were observed at sub-apical locations. Cellular morphology and positioning of the nucleus and centrosome suggest these are delaminated RGPs. Additionally, the radial Golgi morphology found in the VZ of WT was disrupted in Emx1-KO mice (Will et al., 2019). The radial Golgi pattern is associated with the apical process of RGPs (Taverne et al., 2016). The loss of this radial pattern further supports the loss of apical processes in RGPs of Emx1-KO mice (Will et al., 2019). Loss of centrosome components has been shown to lead to similar delamination of RGPs during development (Insolera et al., 2014) and loss of apical RGP endfeet disrupts normal structural integrity of the VS (Shao et al., 2020). It will be interesting to investigate whether Emx1-KO show similar disruptions of the apical membrane. To investigate apical membrane integrity as well as the delamination and mitotic progression over time, immunostainings can be performed at multiple developmental stages. Therefore, I propose to perform immunostaining on E12.5, E14.5 and E16.5 Emx1-WT and Emx1-KO mouse cortices. The staining protocol of the experiments shown in Figure 1 would reveal whether mitotically progressing sub-apical RGPs would increase over time. To study the integrity of the apical membrane, a protocol for en face imaging of the VS (Shao et al., 2020) could be used with immunostaining against α -tubulin, Actin and Pericentrin. In Emx1-KO mice, I expect that the density of apical endfeet would decrease over time. This immunostaining would also provide insight into the MT organization within the apical endfeet.

Single cell labeling of BicD2-depleted RGCs

EVE data further confirms RGP delamination after BicD2 depletion. Additionally, PH3 staining after organotypic slice culture shows the morphology of mitotic RGPs.

Although the same protocol was used for WT and Emx1-KO, the data was obtained in two separate experiments. Therefore, further control experiments must be performed with Emx1-WT and Emx1-KO littermates to allow the quantification of cellular morphology in mitotic RGPs. Moreover, additional immunostaining after EVE can be performed to investigate the location of subcellular structures like the centrosome (anti-Pericentrin) and the Golgi (anti-GM130).

It remains unclear how RGPs release from the VS in Emx1-KO mice. RGPs could lose apical contact after dividing at the VS, or RGPs entering mitosis at sub-apical locations could retract their apical process. Centrosomes were found withing apical processes at large distances from the VS (Fig.1A, arrows), supporting the retraction hypothesis. Here, time-lapse imaging of organotypic slices of Emx1-KO mice, after EVE at E13 could provide more insight into mitotic behavior and the process of delamination in BicD2 depleted RGPs. To investigate centrosome behavior in individual cells, RGPs could be co-transfected with a fluorescent centrosome marker.

Investigation of additional roles of BicD2 in RGPs

The finding that BicD2 immunoreactivity was observed close to Pericentrin-positive punctae at the VS suggests that BicD2 localizes in pericentrosomal punctae in RGPs. This localization could depend on Rab6 binding since Rab6+ vesicles have been shown to accumulate pericentrosomally in cultured cells (Splinter et al., 2012). More recently, Rab6+ vesicle transport was shown to be essential for anchorage of the apical endfoot through apical transport of the polarity protein CRB (Brault et al., 2021). It will be interesting to investigate whether BicD2 positive punctae co-localize with Rab6 at the VS and whether polarity protein organization at the VS is altered. BicD2 positive punctae localized apical to Pericentrin positive punctae. This is surprising because Pericentrin is located apical to the distal appendages of the mother centriole (Shao et al., 2020). Primary cilia are located apically to the centrioles and are essential for apical anchorage of RGPs (Insolera et al. 2014). Therefore, co-staining with primary cilium markers could provide more insight into the exact location of these BicD2 punctae and to the effect of BicD2-depletion on the maintenance of primary cilia.

Interestingly, the data suggests BicD2 positive punctae located to only one of the centrosomes in mitotic nuclei at the VS. Asymmetric inheritance of pericentrosomal proteins is regulated by the maturation of the centrioles where the more mature centriole is inherited by the daughter cell that retains progenitor fate (Wang et al., 2009). The mature mother centriole also stimulates faster primary cilium assembly and attachment to the VS (Anderson et al., 2009). In order to investigate whether BicD2 associates with one of the centrosomes specifically, co-staining could be performed using Pericentrin, BicD2 and the mature centriole specific protein Ninein, together with PV for quantification.

BicD2 variants in human disease

Recently, mutations in BicD2 were shown to be associated with MCD. A C-terminal truncating mutation (K775X) causes lissencephaly, subcortical band heterotopia and

mild hydrocephalus (Tsai et al., 2020). K775X lead to inhibition of BicD2-Nesprin interaction essential for neuronal migration. These results agree with current thinking on the etiology of Lissencephaly and subcortical band heterotopia (Romero et al., 2017). Another mutation (R694C) causes a different pathological phenotype including bilateral perisylvian polymicrogyria (BPP) (Ravenscroft et al., 2016). Both mutations are in the CC3 domain of BicD2 which interacts with cargo proteins including RanBP2 (Splinter et al. 2010), Nesprin (Goncalves et al., 2020) and Rab6 (Grigoriev et al., 2007; Splinter et al., 2012). How these two mutations in the same domain contribute to diverse phenotypes is unclear. Both R694C and K775X are unable to rescue BicD2 depletion during neuronal migration in organotypic culture (Will et al. 2019; Tsai et al., 2020). Interestingly, K775X but not R694C had a dominant negative effect on neuronal migration when expressed in WT organotypic slices (Will et al. 2019; Tsai et al., 2020). This dominant negative effect could explain the difference in phenotype between R694C and K775X. Since both patient mutations are heterozygous and R694C was not dominant negative (Tsai et al., 2020; Ravenscroft et al., 2016), the effect of R694C on neuronal migration might be partially but not fully rescued by the WT allele. This is in line with the hypothesis that polymicrogyria is a neuronal migration disorder (Kato, 2015) and it would suggest that BPP is a milder neuronal migration disorder compared to lissencephaly. In contrast, it has been proposed that polymicrogyria is caused by altered RGP functioning (Romero et al., 2017) and might be caused by a detachment of RGPs (Barkovich et al., 2012). Because the etiology of BPP and the molecular effects of R694C mutations are largely unknown, it has remained unclear what developmental process is affected in patients with R694C mutations. *In vitro* binding essays for these mutant proteins with RanBP2, Nesprin and Rab6 could elucidate the molecular functions affected by R694C mutations. Moreover, the nuclear envelope recruitment and Rab6 co-localization could be analyzed in cultured cells for R694C and K775X compared to WT. In addition, fusion of R694C and WT to a nuclear envelope binding KASH domain could be used as a rescue in neuronal migration assays. If this construct can rescue migration defects in Nex-KO mice, this would indicate that impaired functioning of R694C during neuronal migration is indeed depended on decreased nuclear envelope binding. If delamination can be visualized using EVE as previously discussed, it would be interesting to see whether K775X and R694C mutations would be able to rescue this process in *Emx1*-KO.

In conclusion, here I show that BicD2 is an essential regulator of cell-cycle dependent positioning of RGPs in the developing mammalian neocortex. BicD2-depleted RGPs are impaired in their mitotic progression when the centrosomes are at large distances to the nucleus. Additionally, BicD2 cKO in RGPs causes RGPs detachment from the VS whereafter they continue to divide at sub-apical locations in the presence of perinuclear centrosomes. My results point to unexplored roles for BicD2 in RGPs and provide key insights for further investigation of the pathomechanisms of BicD2 associated neuropathies.

EXPERIMENTAL PROCEDURES

Animals

All applicable institutional, national and international guidelines for the use and care of animals were followed. All experiments with material from mice were performed in compliance with the guidelines for the welfare of experimental animals issued by the Government of The Netherlands, and were approved by the Animal Ethical Review Committee (DEC) of Utrecht University (permit number AVD1080020173404 and 2014.I.03.020)

Antibodies and reagents

Antibodies used in this study: Rabbit anti-BICD2 (HPA023013, Atlas Antibodies) (dil. 1/250); Mouse anti-Pericentrin (611815, BD) (dil. 1/50), Mouse anti-Phospho-Histone H3 (Ser10) (clone nr. 6G3, 9706, Cell Signaling) (dil. 1/500); Rabbit anti-Phospho-Histone H3 (Ser10) (dil. 1/500); Mouse IgG2b anti-Vimentin phospho S55 (clone 4A4, ab22651, Abcam) (dil. 1/50); Rabbit anti-GFP (598, MBL; ab290, Abcam) (dil. 1/500); Alexa488-, Alexa568- and Alexa647-conjugated secondary antibodies (Life Technologies) (dil. 1/500); Other reagents used in this study include: DAPI (Sigma); Fast Green FCF (F7252, Sigma)

Immunohistochemistry

Brains were isolated at E14.5, rinsed with PBS, fixed in paraformaldehyde at 4°C for 2.5h, washed in PBS and transferred to 30% sucrose overnight for cryoprotection prior to freezing in Jung Tissue freezing medium (Leica). Brains were cut in 12 µm coronal sections on a freezing microtome (Leica) and collected on Superfrost Plus™ microscope slides (Thermo Scientific). Sections were washed in PBS, heated in a microwave in Sodium Citrate buffer (10mM, pH6) for 10min at 97°C, washed in PBS and blocked for 1h using 10% normal goat serum in PBS with 0.2% Triton X-100 followed by primary and secondary antibody incubation in blocking solution, both at 4°C overnight. Slides were mounted using Vectashield with DAPI (Vectorlabs) and sealed with nail polish prior to confocal microscopy.

Ex vivo electroporation

Embryonic heads were isolated at E13, and brains were electroporated with 1.5µl DNA mixture containing MARCKS-GFP vector, H2A mKate dissolved in Milli-Q water with 0.05% Fast Green FCF dye (Sigma). DNA mixture was injected in the lateral ventricles of the embryonic brains using a PLI-100A Pico-liter injector (Warner Instruments) and a borosilicate glass micropipettes (World Precision Instruments). Brains were electroporated with platinum plated tweezer-electrodes (Nepagene) using an ECM 830 Electro-Square-Porator (Harvard Apparatus) set to three unipolar pulses at 30V (100ms interval and pulse length). Embryonic brains were isolated and collected in ice-cold cHBSS, embedded in 3% SeaPlaque GTG Agarose (Lonza) in cHBSS and sectioned coronally in 300 µm slices using a VT1000 S Vibratome (Leica). Slices were collected on poly-L-lysine and laminin- coated culture membrane inserts (Falcon), placed on top of slice culture medium (70% v/v Basal Medium Eagle, 26% v/v cHBSS, 20 mM D-Glucose, 1 mM L-Glutamine, 0.1 mg/mL penicillin/streptomycin) and cultured for 1.5 days prior to fixation with 4% paraformaldehyde in PBS. Slices were then blocked and permeabilized in 10% Normal Goat Serum with 0.2% Triton X-100 in PBS followed by primary (anti-GFP, anti-PH3) and secondary antibody incubation (containing DAPI) in blocking solution. Slides were mounted using Vectashield mounting medium with DAPI (Vectorlabs) and sealed with nail polish prior to confocal microscopy.

Immunohistochemistry microscopy

Immunohistochemistry microscopy of cryosections: Confocal laser scanning microscopy was performed using a LSM-700 system (Zeiss) with a Plan-Apochromat 20x NA 0.8, an EC Plan-Neofluar 40x NA1.30 Oil DIC Plan- Apochromat, or a Plan-Apochromat 63x NA 1.40 oil DIC. Z-stacks were selected to

cover the entire section and taken in software (ZEN) suggested optimal size steps. Immunohistochemistry microscopy of fixed organotypical slice cultures after ex vivo electroporation: Confocal laser scanning microscopy was performed using a LSM-700 system (Zeiss) with a Plan-Apochromat 20x NA 0.8 objective or using a SP8 system (Leica) with a HCX PL FLUOTAR L 20x objective. Z-stacks were selected to cover the entire section and taken in software (ZEN) suggested optimal size steps.

Image analysis and quantification

Linear image processing and analysis was performed in FIJI. All quantifications were performed using the same microscope settings across experiments.

Mitotic progression

The condensation state of chromatin was determined using DAPI staining. The presence of perinuclear centrosomes was determined by Pericentrin staining within the phospho-vimentin positive area surrounding the nucleus. Mitotic cells were counted as apical when the nucleus was within 30µm of the Ventricular surface and as sub-apical otherwise. Centrosomes were counted using cell-counter in the centrosome poor regions in the outer ventricular zone. Cleavage plane orientation was determined using the angle tool, measuring the angle between the radial direction of the cortex and a line connecting the two centrosomes.

Statistical analysis

All statistical details of experiments can be found in figure legends. All data was checked for normality by Shapiro–Wilk test. I define the number of mice as N and the number of counted cells/individual data points as n. Data processing and statistical analysis were done in Excel and GraphPad Prism 7. Significance was defined as: ns=not significant or $p > 0.05$, * for $p < 0.05$, ** for $p < 0.005$, *** for $p < 0.001$. Error bars are \pm SEM.

ACKNOWLEDGEMENTS

I would like to thank Lena Will for her supervision, guidance, support, feedback and her patience. Merel van Luyk, thank you for cooperation and many discussions. Sybren Portegies, thank you for guidance and help. I would like to thank Casper Hoogenraad for working in his lab. And I would like to thank Esther de Graaff for examining the final report. This work was supported by the Netherlands Organization for Scientific Research (NWO-ALW-VICI, CCH), the Netherlands Organization for Health Research and Development (ZonMW-TOP, CCH), the European Research Council (ERC) (ERC-consolidator, CCH) and the Internationale Stichting Alzheimer onderzoek (ISAO, D.J.).

AUTHOR CONTRIBUTION

Experiments shown in this report were conceptualized, performed and analyzed by J.J. van Schelt. Figure design of figure 1 by J.J. van Schelt with help of S. Portegies.

Contribution to Will et al., 2019:

- Westernblots (Figure S1): Co-performed with M. van Luyk and analyzed by J.J. van Schelt.
- CAS3/NeuN stainings (Figure 5): Performed and co-analyzed (all counting) by J.J. van Schelt.
- PAX6/PH3/TBR2 stainings (Figure 6): co-analyzed (all counting) by J.J. van Schelt

REFERENCES

Anderson, C.T. & Stearns, T. (2009). Centriole age underlies asynchronous primary cilium growth in mammalian cells. *Current Biology*, 9(17), 1498-1502. <https://doi.org/10.1016/j.cub.2009.07.034>

Baffet, A., Hu, D. & Vallee, R.B. (2015). Cdk1 activates pre-mitotic nuclear envelope dynein recruitment and apical nuclear migration in neural stem cells. *Developmental Cell*, 33(6), 703-716. <https://doi.org/10.1016/j.devcel.2015.04.022>

Barkovich A.J., Guerrini, R., Kuzniecky, R.I., Jackson, G.D., W.B. Dobyns, W.B., (2012). A developmental and genetic classification for malformations of cortical development: update 2012. *Brain Journal of Neurology*. 135 1348–1369. <http://dx.doi.org/10.1093/brain/aws019>

Bertapaglia, C., Gonçalves, J. C., & Vallee, R. B. (2017). Nuclear migration in mammalian brain development. *Seminars in Cell and Developmental Biology*. 82, 57-66. <http://doi.org/10.1016/j.semcdb.2017.11.033>

Brault, J.B., Bardin, S., Lampic, M., Carpentieri, J.A., Coquand, L., Penisson, M., et al. (2021). bioRxiv. <https://doi.org/10.1101/2021.07.23.453475>

Goncalves, J.C., Quintremil, S., Yi, J. & Vallee, R.B. (2020). Nesprin-2 Recruitment of BicD2 to the Nuclear Envelope Controls Dynein/Kinesin-Mediated Neuronal Migration In Vivo. *Current Biology*, 30(16), 3116-3129. <https://doi.org/10.1016/j.cub.2020.05.091>

Grigoriev, I., Splinter, D., Keijzer, N., Wulf, P.S., Demmers, J., Ohtsuka, T., et al. (2007). Rab6 regulates transport and targeting of exocytotic carriers. *Developmental Cell*, 13(2), 305-314. <https://doi.org/10.1016/j.devcel.2007.06.010>

Hu, D.J., Baffet, A.D., Nayak, T., Akhmanova, A., Doye, V., & Vallee, R. B. (2013). Dynein recruitment to nuclear pores activates apical nuclear migration and mitotic entry in brain progenitor cells. *Cell*, 154(6), 1300-1313. <https://doi.org/10.1016/j.cell.2013.08.024>

Insolera, R., Bazzi, H., Shao, W., Anderson, K.V. & Shi, S. (2014). Cortical neurogenesis in the absence of centrioles. *Nature Neuroscience*, 17 (11), 1528-1535. <https://doi.org/10.1038/nn.3831>

Jaarsma, D., van den Berg, R., Wulf, P.S., van Erp, S., Keijzer, N., Schlager, M.A., et al. (2014). A role for bicaudal-D2 in radial cerebellar granule cell migration. *Nature Communications* [E], 5, 3411. <https://doi.org/10.1038/ncomms4411>

Kato, M. (2015). Genotype-phenotype correlation in neuronal migration disorders and cortical dysplasias. *Frontiers in Neuroscience*, 9, 181. <https://doi.org/10.3389/fnins.2015.00181>

Kriegstein, A., & Alvarez-Buylla, A. (2009). The Glial nature of embryonic and adult neural stem cell. *Annual Review of Neuroscience*, 32(1), 149-184. <https://doi.org/10.1146/annurev.neuro.051508.135600>

Neveling, K., Martinez-Carrera, L., Hölker, I., Heister, A., Verrips, A., Hosseini-Barkoobe, S.M., et al. (2013). Mutations in BICD2, which encodes a golgin and important motor adaptor, cause congenital autosomal-dominant spinal muscular atrophy. *American Journal of Human Genetics*, 92(6), 946-954. <https://doi.org/10.1016/j.ajhg.2013.04.011>

Noctor, S.C., Flint A.C., Weissman, T. A., Dammerman, R.S., Kriegstein, A. R. (2001). Neurons derived from radial glial cells establish radial units in neocortex. *Nature*. 409, 714–20. <https://doi.org.proxy.library.uu.nl/10.1038/35055553>

Noctor, S.C., Martínez-Cerdeño, V., Ivic, L. & Kriegstein, A.R. (2004). Cortical neurons arise in symmetric and asymmetric division zones and migrate through specific phases. *Neuroscience*, 7 (2), 136-144. <https://doi.org/10.1038/nn1172>

Peeters, K., Litvinenko, I., Asselbergh, B., Almeida-Souza, L., Chamova, T., Geuens, T., et al. (2013). Molecular defects in the motor adaptor BICD2 cause proximal spinal muscular atrophy with autosomal-dominant inheritance. *The American Journal of Human Genetics*, 92(6), 955-964. <https://doi.org/10.1016/j.ajhg.2013.04.013>

Ravenscroft, G., Donato, N.D., Hahn, G., Davis, M.R., Craven, P.D., Poke, G., et al. (2016). Recurrent de novo BICD2 mutation associated with arthrogryposis multiplex congenita and bilateral perisylvian polymicrogyria. *Neuromuscular Disorders*, 26, 744- 748. <https://doi.org/10.1016/j.nmd.2016.09.009>

Shitamukai, A., Konno, D., & Matsuzaki, F. (2011). Oblique radial glial divisions in the developing mouse neocortex induce self-renewing progenitors outside the germinal zone that resemble primate outer subventricular zone progenitors. *The Journal of Neuroscience*, 31(10), 3683. <https://doi.org/10.1523/JNEUROSCI.4773-10.2011>

Splinter, D., Tanenbaum, M., Lindqvist, A., Jaarsma, D., Flotho, A., Yu, K. L., et al. (2010). Bicaudal D2, dynein, and kinesin-1 associate with nuclear pore complexes and regulate centrosome and nuclear positioning

- during mitotic entry. *PLoS Biology*, 8(4), e1000350. <https://doi.org/10.1371/journal.pbio.1000350>
- Shao, W., Yang, J., He, M., Yu, X., Lee, C.H., Yang, Z., et al. (2020). Centrosome anchoring regulates progenitor properties and cortical formation. *Nature*, 580, 106-112. <https://doi.org/10.1038/s41586-020-2139-6>
- Splinter, D., Razafsky, D., Schlager, M., Serra-Marques, A., Grigoriev, I., Demmers, J., et al. (2012). BICD2, dynactin, and LIS1 cooperate in regulating dynein recruitment to cellular structures. *Molecular Biology of the Cell*, 23(21), 4226-4241. <https://doi.org/10.1091/mbc.e12-03-0210>
- Taverna, E., Mora-Bermúdez, F., Stryz, P.J., Florio, M., Icha, J., Haffner, C., et al. (2016). Non-canonical features of the Golgi apparatus in bipolar epithelial neural stem cells. *Nature scientific reports*, 6, 21206. <http://doi.org/10.1038/srep21206>
- Tsai, M., Cheng, H., Nian, F., Liu, C., Chao, N., Chiang, K., et al. (2020). Impairment in dynein-mediated nuclear translocation by BICD2 C-terminal truncation leads to neuronal migration defect and human brain malformation. *Acta Neuropathologica Communications*, 8, 106. <https://doi.org/10.1186/s40478-020-00971-0>
- Tsai, J., Vallee, R. B., Lian, W., Kriegstein, A. R., & Kemal, S. (2010). Kinesin 3 and cytoplasmic dynein mediate interkinetic nuclear migration in neural stem cells. *Nature Neuroscience*, 13 (12), 1463-1471. <https://doi.org/10.1038/nn.2665>
- Wang, X., Tsai, J., Imai, J.H., Lian, W., Lian, W., Vallee, R.B. & Shi, S. (2009). Asymmetric centrosome inheritance maintains neural progenitors in the neocortex. *Nature*, 461, 947-955. <https://doi-org.proxy.library.uu.nl/10.1038/nature08435>
- Will, L., Portegies, S., van Schelt, J.J., van Luyk, M., Jaarsma, D., Hoogenraad, C.C. (2020). Dynein activating adaptor BICD2 controls radial migration of upper-layercortical neurons in vivo. *Acta Neuropathologica Communications* 7, 162. <https://doi.org/10.1186/s40478-019-0827-y>